# Adipose tissue-derived stem cell-seeded small intestinal submucosa for tunica albuginea grafting and reconstruction

Limin Ma[a,b,1], Yijun Yang[a,1], Suresh C. Sikka[a,c], Philip J. Kadowitz[c], Louis J. Ignarro[d], Asim B. Abdel-Mageed[a,c,2], and Wayne J. G. Hellstrom[a,2,3]

Departments of [a]Urology and [c]Pharmacology, Tulane University Health Sciences Center, New Orleans, LA 70112; [b]Department of Urology, Ninth People's Hospital Affiliated with Medical College of Shanghai, Jiaotong University, Shanghai 200011, China; and [d]Department of Molecular and Medical Pharmacology, David Geffen School of Medicine, University of California, Los Angeles Center for the Health Sciences, Los Angeles, CA 90095

Edited by Solomon H. Snyder, The Johns Hopkins University School of Medicine, Baltimore, MD, and approved December 13, 2011 (received for review August 29, 2011)

**Porcine small intestinal submucosa (SIS) has been widely used in tunica albuginea (TA) reconstructive surgery. Adipose tissue-derived stem cells (ADSCs) can repair damaged tissue, augment cellular differentiation, and stimulate release of multiple growth factors. The aim of this rat study was to assess the feasibility of seeding ADSCs onto SIS grafts for TA reconstruction. Here, we demonstrate that seeding syngeneic ADSCs onto SIS grafts (SIS-ADSC) resulted in significant cavernosal tissue preservation and maintained erectile responses, similar to controls, in a rat model of bilateral incision of TA, compared with sham-operated animals and rats grafted with SIS graft (SIS) alone. In addition to increased TGF-β1 and FGF-2 expression levels, cross-sectional studies of the rat penis with SIS and SIS-ADSC revealed mild to moderate fibrosis and an increase of 30% and 40% in mean diameter in flaccid and erectile states, respectively. SIS grafting induced transcriptional up-regulation of iNOS and down-regulation of endothelial NOS, neuronal NOS, and VEGF, an effect that was restored by seeding ADCSs on the SIS graft. Taken together, these data show that rats undergoing TA incision with autologous SIS-ADSC grafts maintained better erectile function compared with animals grafted with SIS alone. This study suggests that SIS-ADSC grafting can be successfully used for TA reconstruction procedures and can restore erectile function.**

Peyronie's disease | incision and grafting procedures | penile surgery

The veno-occlusive mechanism responsible for erection intimately depends on the extensibility, rigidity, and compliance of the tunica albuginea (TA) (1). Any morphological or functional impairment or defect in the TA can affect compliance of the penile fibro-elastic framework and have profound effects on the hemodynamic and erectile function of the penis (2). TA reconstruction is often used in Peyronie's disease (PD) with large plaques, severe deformities, or short penises that require incision or excision for placement of grafts to augment or lengthen the penis (3). There are myriad different autologous graft tissues harvested from the patient's body, such as dermis, temporalis fascia, tunica vaginalis, penile skin, and saphenous vein, as well as cadaveric tissues, such as dermis, fascia, pericardium, and porcine small intestine submucosa. A number of synthetic materials such as Gore-Tex, Dacron, and silastic mesh have been used for grafting procedures (4). Erectile dysfunction (ED), recurrence of penile curvature, and penile shortening are recognized complications from such grafting procedures (4).

Mesenchymal stem cells (MSCs) are a well-characterized population of adult stem cells capable of self-renewal. Based on their plasticity, several lines of evidence demonstrate that MSCs have the potential to engraft and differentiate into multiple lineages both in vitro and in vivo (5). The growing interest in the use of MSCs in regenerative medicine and tissue reconstruction is explained, in part, by the relative ease of their isolation from several adult human tissues, propagation in culture, and their differentiation capacity. Using tissue-engineering techniques, the clinical utility of stem cell transplantation has been demonstrated in vascular (6) and cartilage reconstruction (7) and in restoring immune response and hematopoiesis (8). In vivo scaffold-based studies further expanded the use of MSCs in new bone formation (9).

With the development of tissue engineering, cell-seeded acellular matrix grafts can theoretically provide off-the-shelf reconstructive materials. Although it has been demonstrated for tissue reconstruction in other clinical settings, there are no studies investigating the therapeutic efficacy of such materials in procedures involving surgical intervention of the TA. SIS has been widely used in the reconstruction of various tissues and organs (10). As with MSCs, ADSCs have the potential to restore damaged tissue and prevent some of the above-mentioned postoperative problems. The aim of this study was to assess the feasibility of the use of ADSC-seeded SIS grafts for reconstruction of bilaterally incised TA in a rat model. The hypothesis that ADSC seeding onto SIS will maintain erectile function was also examined.

## Results

**ADSCs Culture, Characterization, and BrdU Labeling.** The ADSC isolates attached and proliferated within 2–3 d and were passaged when they reached 80% confluence. ADSCs became fusiform and exhibited spindle-shaped morphologies (Fig. 1*A*). Flow cytometric analysis demonstrated that ADSCs (passage 3–5) were positive for CD29 (97.62%), CD90 (92.21%), and CD105 (15.87%), but negative for CD45 (4.37%) expression (Fig. 1*B*). To assess engraftment of ADCSs onto SIS, cells were efficiently (>95%) labeled with antibromodeoxyuridine (BrdU; Sigma) antibody in vitro (Fig. 1*C*).

**Seeding of ADSCs onto the SIS Grafts.** A four-layer porcine SIS was provided as a soft tissue graft (Surgisis ES) from Cook Medical (Bloomington, IN). Based on histological examination, SIS is an acellular nondirected fibrous material (Fig. 2*A*). The ADSC-seeded SIS grafts were cultured in an air fluid media for 1 wk. Random H&E staining revealed that ADSCs grew well, attached onto the SIS, exhibited a similar cellular morphology, and formed multilayer epithelium on the SIS scaffolds (Fig. 2*B*).

**Measurement of Erectile Responses.** The SIS and SIS-ADSC were surgically implanted into the rat penis (Fig. 2 *C–F*). Erectile

Author contributions: L.M., Y.Y., A.B.A.-M., and W.J.G.H. designed research; L.M. and Y.Y. performed research; S.C.S., P.J.K., and L.J.I. analyzed data; and S.C.S., P.J.K., A.B.A.-M., and W.J.G.H. wrote the paper.

The authors declare no conflict of interest.

This article is a PNAS Direct Submission.

[1]L.M. and Y.Y. contributed equally to this work.

[2]A.B.A.-M. and W.J.G.H. contributed equally to this work.

[3]To whom correspondence should be addressed. E-mail: whellst@tulane.edu.

This article contains supporting information online at www.pnas.org/lookup/suppl/doi:10.1073/pnas.1113810109/-/DCSupplemental.

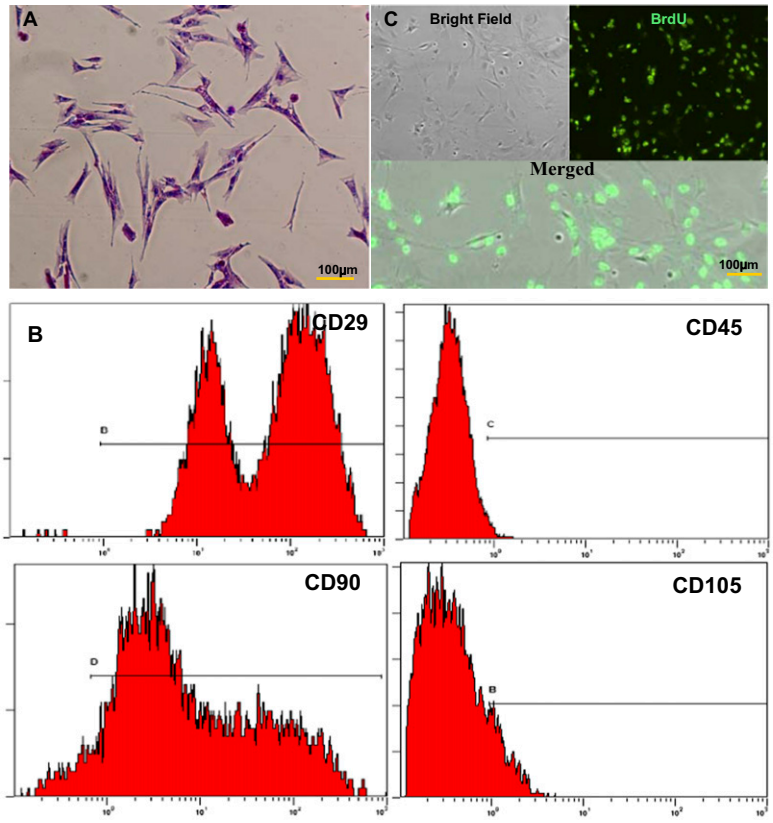


**Fig. 1.** Identification and BrdU labeling of ADSCs. (*A*) Methyl violet staining of ADSCs. (Scale bar: 100 μm.) (*B*) Flow cytometric analysis of early passage rat ADSCs with positive expression for CD29 (97.62%), CD90 (92.21%), and CD105 (15.87%) and low expression of CD45 (4.37%). (*C*) Immunofluorescence to calculate the labeling index (positive rate) of ADSCs incubated with BrdU at 20 μmol/L for 48 h. The nuclei of ADSCs showed green fluorescence, and the labeling rate exceeded 95%.

responses were examined 8 wk after surgical intervention. Fig. 3*A* shows maximum increase in intracavernosal pressure (ICP), ICP/mean arterial pressure (MAP), and total ICP values in response to cavernous nerve stimulation (CNS) for 1 min in control groups in a voltage-dependent manner. Conversely, erectile responses in rats with the SIS were significantly lower ($P < 0.05$) (Fig. 3 *B–D*). Similar to controls, seeding ADSCs on the SIS grafts resulted in a significant restoration of the erectile function compared with SIS group ($P < 0.05$) (Fig. 3 *B–D*).

**Penile Measurements and Histological Assessment.** We measured the diameter and length of the rat penis in the four surgical groups to illustrate the properties of the SIS. Compared with the sham group, rats with SIS-ADSC and SIS revealed 40% and 30% increase in mean diameter under flaccid and erectile states, respectively ($P < 0.001$) (Fig. 4*A*). We also observed no significant difference in all groups in mean penile length under either flaccid or erectile conditions (Fig. 4*B*).

In the BrdU immunostained frozen penile sections grafted SIS-ADSC, a weak signal on the surface of the graft and slight sporadic reactivity on the corpus cavernosum were detected (Fig. 4*B*). Masson's trichrome staining of the TA of control (Fig. 4*C*) and sham-operated rats (Fig. 4*D*) revealed numerous collagen bundles oriented in two directions with an abundance of elastic fibers. In the SIS group (Fig. 4*E*) there was moderate fibrosis under the graft and a mild foreign-body reaction around the suture. In the SIS-ADSC group (Fig. 4*F*), only mild fibrosis was observed around the graft, and the elastic fibers of the graft were orientated in two layers, similar to the adjacent TA. The assessed penile fibrosis score of the SIS group was significantly greater compared with the other three groups (Fig. 4*G*).

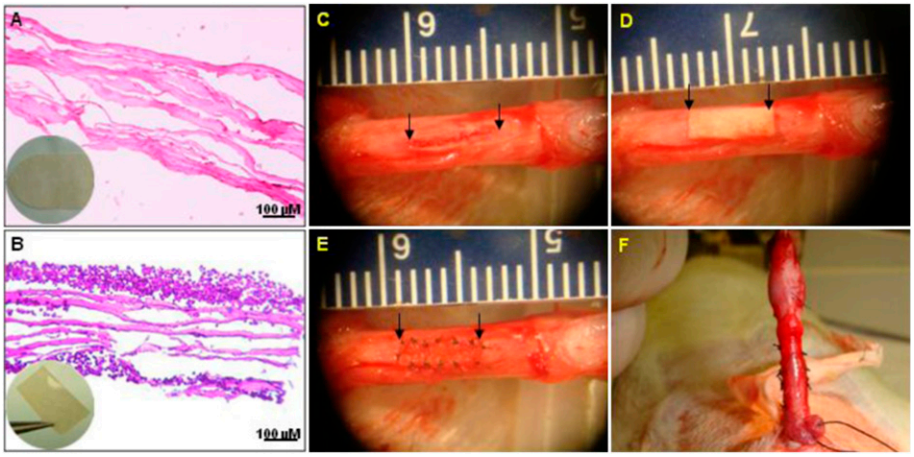


**Fig. 2.** SIS-ADSC grafts and reconstruction surgery of TA. (*A*) Four-layer SIS showed nondirected fibers, which were completely acellular. (*B*) H&E staining demonstrated that ADSCs engrafted and formed multiple layers on the SIS scaffolds. (*C*) Rat penis middle section was chosen as the surgery site. Rats underwent first stage surgery, which included a 5-mm incision (arrows) on both sides of the TA. (*D* and *E*) A 10 $mm^2$ SIS and stem cell-seeded SIS (arrow) was interpositioned and sutured with 8-0 nylon for the third or fourth groups. (*F*) All excisions for tunica grafting were performed laterally to protect the dorsal cavernous nerves from injuries.

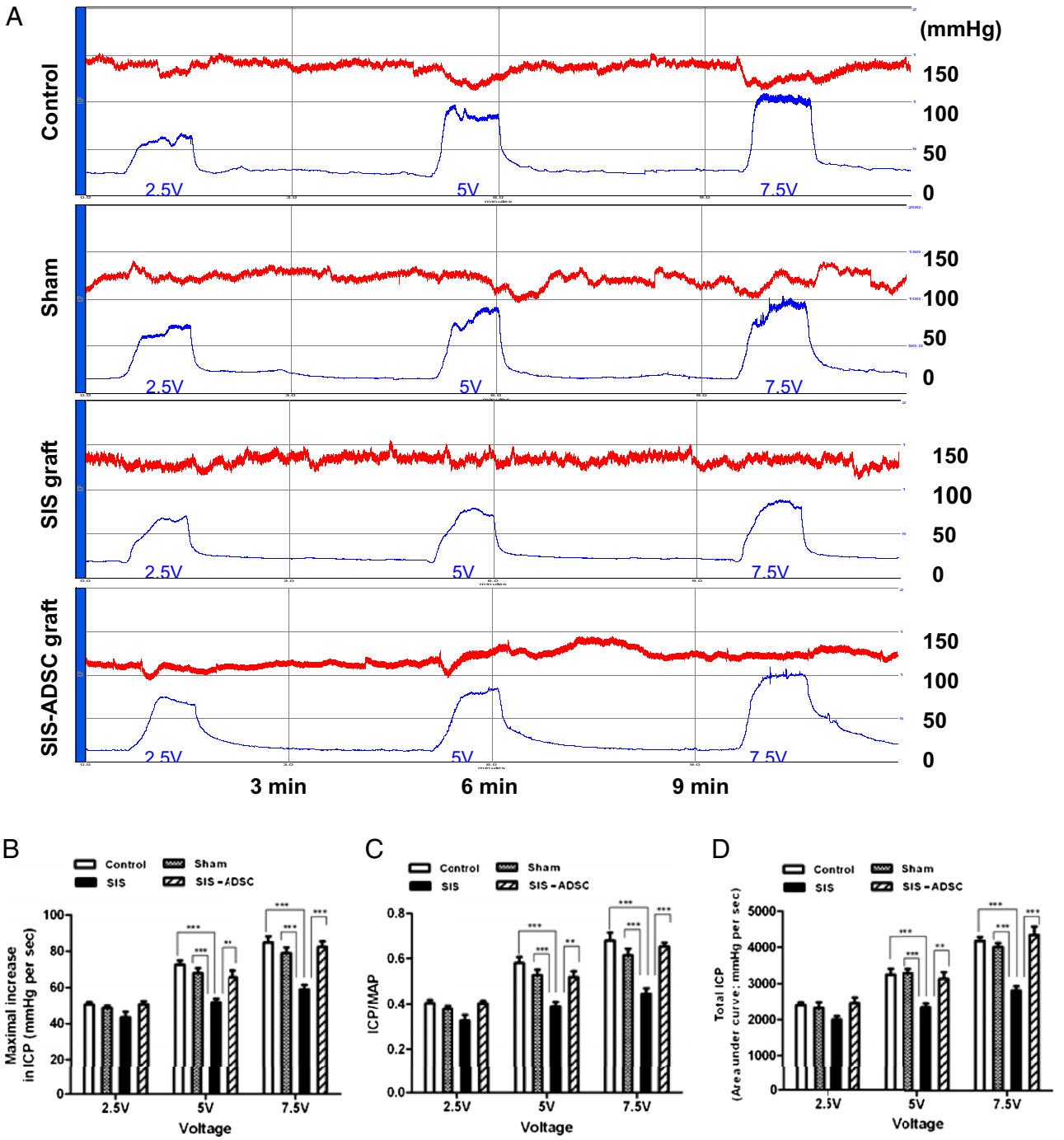


**Fig. 3.** Evaluation of erectile function response to cavernosal nerve electrostimulation. (*A*) Representative ICP (blue curve) and MAP (red curve) tracing after CNS as described in *Materials and Methods*. Total erectile response (ICP) was determined by measuring the AUC in millimeter of mercury per second from the beginning of CNS until ICP returned to baseline or prestimulation pressure. The ratio of maximal ICP-to-MAP was determined relative to controls for variations in systemic blood pressure. (*B–D*) Maximal increase in ICP, ICP/MAP, and total ICP values in response to CNS with different voltage settings. $n = 8$ individual experiments per condition; Mean ± SE are reported; $^{*}P < 0.05$; $^{**}P < 0.01$; and $^{***}P < 0.001$.

**Expression Profile of NOS Isoforms and Fibrosis-Related Factors in Grafted Penile Tissue.** We investigated the middle of the graft site with or without ADSCs by using immunostaining with anti-NOS antibodies. The overall NOS expression was illustrated by photomicrographs of selected areas of the corpora cavernosa (Fig. 5 *A*, *B*, and *D*) and the dorsal cavernous nerves (Fig. 5*C*). Unlike in the SIS rats, endothelial NOS (eNOS) was significantly high in the corpus cavernosum of the control, sham operated, and SIS-ADSC groups (Fig. 5*A*). Similar pattern of neuronal NOS (nNOS) staining was observed in the corpus cavernosum and in the dorsal nerves (Fig. 5 *B* and *C*). Inducible NOS (iNOS) protein expression was weak in the control group compared with the other three groups, with the highest staining in the SIS group (Fig. 5*D*). nNOS expression was detected in dorsal cavernous nerves (Fig. 5*C*) and, to a lesser extent, in corpora cavernosa (Fig. 5*B*). Localization analyses of NOS proteins have characterized presence of iNOS in the nucleus, nNOS in nerve cell cytoplasm, and eNOS in the cytoplasm of endothelial cells. The exhibited characteristics and tissue-specific

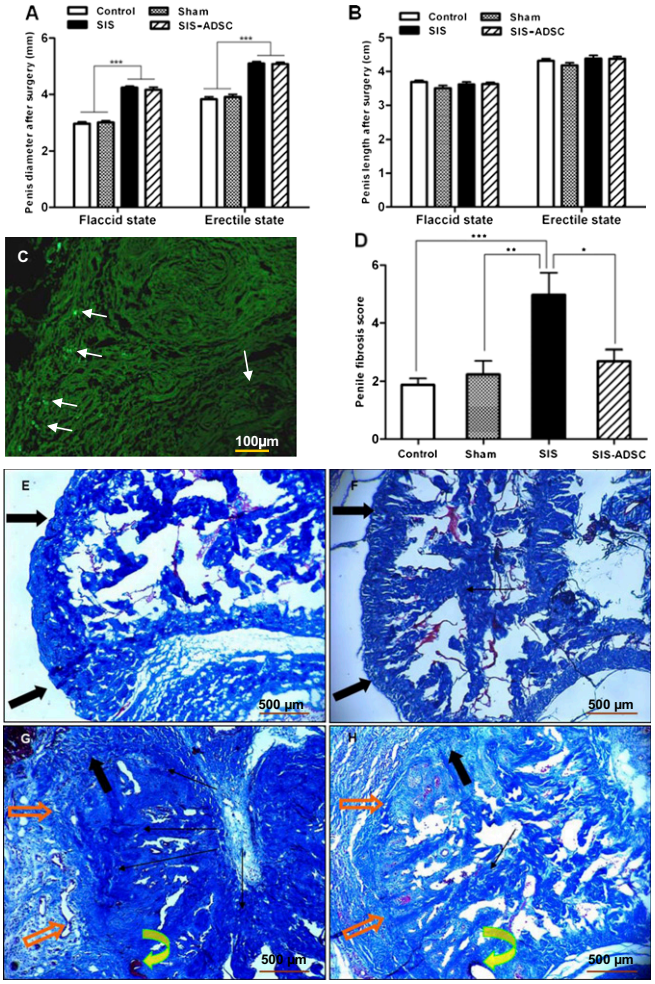


**Fig. 4.** Morphology and histological assessment of penile tissue cross-sections. (*A*) Compared with the sham group, rats with SIS graft with or without ADSCs seeding revealed ≈38.2–41.0% and 29.5–30% increases in mean penile diameter under flaccid and rigid conditions, respectively. The penile length was not affected by grafting (*B*). (*C*) Fluorescent signal from the BrdU-labeled ADSCs (arrows) can be detected on the surface of the graft and in the corpus cavernosum. Penile fibrosis score of SIS graft was significantly high compared with other experimental groups (*D*). Masson's trichrome staining (40×) in the TA of control (*E*) and sham-operated rats (*F*) after 8 wk showed numerous collagen bundles orientated in two directions (inner circular and outer longitudinal) with an abundance of elastic fibers. (*G*) Moderate fibrosis under the graft and a mild foreign-body reaction around the suture in the SIS group. In the SIS-ADSC group (*H*), only mild fibrosis was present around the graft, and the elastic fibers of the graft were orientated in two layers, similar to the adjacent tunica albuginea. Orange arrows indicate SIS graft, curved yellow arrows show the suture, solid black arrows depict the normal TA, and lined black arrows denote fibrosis. $n = 8$ per condition, Mean ± SE are reported. $^{*}P < 0.05$, $^{**}P < 0.01$, and $^{***}P < 0.001$.

expression of NOS were verified by the negative staining of endothelial cell and smooth muscle cell markers.

We characterized by quantitative RT-PCR (qRT-PCR) the expression of prominent genes involved in functional erection and fibrosis in rat penile tissue. Whereas the SIS-ADSC graft restored the expression of the eNOS (Fig. 6*A*) and nNOS (Fig. 6*B*) transcripts, they were significantly decreased in the SIS group. However, iNOS gene expression increased significantly in the SIS rats, which then decreased upon seeding ADSCs on the SIS graft (Fig. 6*C*). The expression pattern of NOS and fibrosis-related genes in penile tissues was confirmed by Western blot analysis (Fig. 6 *G* and *H*).

Next, we investigated the expression profiles of fibrosis-related factors in penile tissues. The VEGF expression decreased significantly in the SIS group, whereas SIS-ADSC graft resulted in restoration of VEGF expression (Fig. 6 *D*, *I*, and *J*). Although the SIS rats had the highest expression level, SIS-ADSC grafting resulted in a moderate yet significant increase in TGF-β1 expression ($P < 0.05$) compared with controls (Fig. 6 *E*, *I*, and *J*). FGF-2 transcripts increased in both grafted groups compared with controls ($P < 0.05$) (Fig. 6 *F*, *I*, and *J*).

## Discussion

With tissue engineering, cell-seeded acellular matrix grafts have achieved prominence as a potential off-the-shelf replacement material. This material is moving from bench to bedside for reconstruction of the urethra, testis, and bladder. However, there are no similar reports for PD and TA reconstruction. Promising results showed an 80–95% success rate using the Surgisis ES SIS (ES Cook) grafting for TA reconstruction (11). However, another report questioned the efficacy of grafting with SIS, because there were recurrences of curvature in three of four patients (12).

Porcine SIS is a resorbable stratum compactum layer of tunica mucosa, tunica muscularis mucosa, and submucosa, which is rich in several types of collagen, fibronectin, FGF, and TGF-β, which all contribute to wound healing, cell signaling, and tissue remodeling (13). Being acellular and immunocompatible, it elicits only minor or no antigenic responses. SIS, unlike other available acellular matrix grafts, such as gluteraldehyde-treated bovine and cadaveric pericardium, is resorbable because it is not cross-linked. SIS tensile strength increases over time, which is important in any TA reconstruction procedure to prevent bulging, aneurysmal dilatation, and veno-occlusive dysfunction (4).

Various MSCs derived from fat, bone marrow, and umbilical cord blood have received attention in the field of tissue engineering because of their distinct biologic capability to differentiate into specialized cell types (14). The stromal vascular fraction of adipose tissue contains multipotent progenitor cells (ADSCs) that are capable of differentiating into mesenchymal tissue (15). Compared with other MSCs, ADSCs can easily be harvested from patients and can be cultured and expanded rapidly. In addition, long-term cultured ADSCs retain their mesenchymal pluripotency (16). In this study, we confirmed that the donor rat ADSCs not only express characteristic surface markers (CD29, CD90, and CD105 positive, and CD45 negative) but also exhibit multilineage potential of MSCs.

Clinically, ED secondary to venous leak can develop in 5–30% of men undergoing surgical treatment for PD (4). Our study shows that rats undergoing TA incision and grafting with autologous ADSC-seeded SIS have significantly less ED, compared with SIS-grafted rats. Autologous ADSCs have been shown to improve recovery of erectile function in rat model cavernous nerve injury (17). Thus, ADSCs can improve erectile function as was demonstrated in the present study.

The in vivo long-term survival of ADSCs was evident by detection of BrdU immunoreactivity on the surface of the graft and in the corpus cavernosum 8 wk after surgery in the grafted rats. However, the mechanism for the beneficial effects of ADSCs in erectile function is complex. Fibrosis interferes with the compliance of the corporal tissues after stimulation by the nitric oxide (NO)/cGMP system (18). In this study, Masson's trichrome staining at 8 wk revealed minimal fibrosis in controls and SIS-ADSC graft compared with SIS group. A loss of smooth muscle cells, increased expression of TGF-β1, excessive deposition of collagen fibers, and extracellular matrix were observed in the corpora of the SIS graft model. Because fibrosis can be reduced by TGF-β blockade (19), we assumed that fibrosis may diminish blood flow to the corpora during tumescence. Our results suggest ADSCs accelerate recovery of the TA and underlying corpora cavernosal tissue by inhibiting fibrosis and enhancing angiogenesis. This finding is consistent with the fact that ADSCs secrete bioactive levels of angiogenic factors, such as VEGF and hepatocyte growth factor (HGF) (20), especially under hypoxic conditions (21). Conversely, HGF-targeted silencing in ADSCs reduces their proangiogenic effects and ability to promote endothelial cell proliferation (22). Tissue restoration and increased angiogenesis may also be attributed to up-regulation of iNOS in

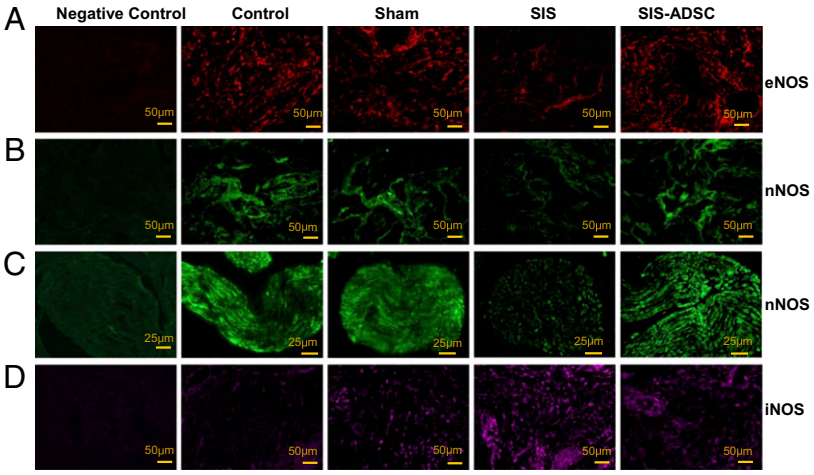


**Fig. 5.** Immunofluorescence staining of NOS family in the corpus cavernosum of control, sham-operated, SIS, and SIS-ADSC groups. Positive immunostaining was observed in the corpus cavernosum (*A*, *B*, and *D*) and dorsal nerves (*C*) of the rat penis. Staining of eNOS and nNOS showed diffuse but marked staining in the corpus cavernosum of the control, sham operated, and SIS-ADSC groups, whereas weak staining was detected in the SIS group. Weak nNOS immunoreactivity was detected in the dorsal nerves of the SIS rats compared with the other groups. However, intense immunostaining of iNOS was noticed in corpus cavernosum of the surgical groups, with highest levels detected in the SIS group, compared with controls. Tissue sections processed without primary antibodies served as negative controls.

SIS-ADSC–grafted TA. Increased tissue survival resulting from iNOS-dependent enhancement of VEGF levels and an ensuing angiogenic response has been reported (23). These findings suggest that the SIS-ADSC grafts may contribute to tissue restoration by enhancing angiogenesis directly or indirectly.

NO released from nitrergic nerves play an important role in initiating trabecular smooth muscle relaxation and penile erection. In this study, results of qRT-PCR, immunofluorescence, and immunoblot analyses show that SIS-ADSC grafts are accompanied by increased expression of eNOS, nNOS, and reduced expression of iNOS in both dorsal nerves and cavernosal tissue. We showed up-regulation of iNOS causes ED in a rat model of bilateral cavernous nerve crush injury (24). Furthermore, iNOS inhibition has been shown to improve erectile response via alteration of the vascular tone of the penis (25). In type II diabetic rats, down-regulation of eNOS and nNOS was associated with apoptosis-induced erectile tissue damage (26). These findings suggest that ADSCs may produce an important restorative effect on constitutive NOS expression.

Of interest, SIS grafting with or without ADSCs produces obvious girth enhancement in the penis, indicating that SIS has an effective anticontractile effect. This improvement was clearly evident by measurement of penile diameter under flaccid and rigid conditions in vivo. Considering that ED and recurrence of curvature caused by graft shrinkage are common postoperative adverse effects after PD surgery, the results of this study suggest that SIS-ADSC approach may have potential clinical implications for grafting and reconstruction of the TA.

## Materials and Methods

**Rat ADSCs Isolation and Culture.** ADSCs were harvested from inguinal fat tissue of adult male Sprague–Dawley (SD) rats (400–450 g; Charles River) by using an

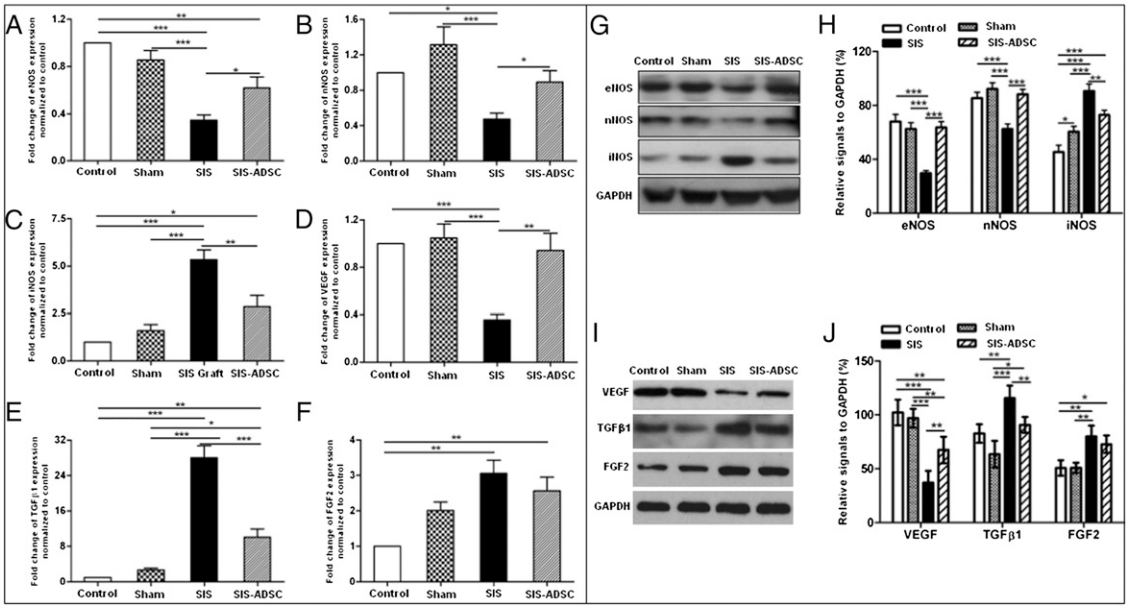


**Fig. 6.** qRT-PCR and immunoblot analysis of NOS isoforms and erectile function related factors. Compared with both the control and sham groups, mRNA levels of the eNOS (*A*), nNOS (*B*) and VEGF (*D*) decreased significantly in the SIS group. However, their expression was restored in the SIS-ADSC group. iNOS (*C*) and TGF-β1 (*E*) transcripts increased significantly in the SIS rats, whereas seeding ADSCs on SIS grafts down-regulated their expression. (*F*) FGF-2 transcripts significantly elevated in the SIS and SIS-ADSC groups in comparison with the controls. (*G* and *H*) A representative blot of the respective proteins depicting decreased levels of eNOS and nNOS proteins and an increase in iNOS protein expression in the SIS graft group in comparison with other groups. (*I* and *J*) TGFβ1 and FGF2 protein levels were significantly increased whereas VEGF protein expression significantly decreased in the SIS and SIS-ADSC groups in comparison with controls. All experiments were repeated three times. $n = 8$ per condition; Mean ± SE are reported; $^{*}P < 0.05$, $^{**}P < 0.01$, and $^{***}P < 0.001$.

Institutional Animal Care and Use Committee approved protocol. A lower midline abdominal skin incision was made, and fat pads around the spermatic cord were excised, finely minced, and washed three times with PBS containing penicillin (100 units per mL) and of streptomycin (100 μg/mL). After centrifugation (500 × g; 5 min) tissue samples were digested with collagenase type 1 (0.2%, Invitrogen) by agitation at 37 °C for 90 min. After filtration through a 200-μm nylon mesh, ADSCs were resuspended and cultured at a density of $1 \times 10^5$ cells in DMEM+F12 medium supplemented with 10% FBS (GIBCO BRL) and antibiotics. Nonadherent cells were removed 2 d after culture, and medium was then changed every 3 d until 85–95% confluence.

**Flow Cytometry.** The ADSC (passage 3) were evaluated for viability and stained for analytical flow cytometry (27). Briefly, $2 \times 10^5$ cells in PBS containing 0.2% FCS were incubated with anti-rat or -mouse monoclonal antibodies for CD29, CD45, CD90, and CD105 (BD Biosciences) conjugated with either phycoerythrin (PE) or fluorescein isothiocyanate (FITC) in 50 μL of PBS for 30 min in the dark at 4 °C. After washing, cells were analyzed on a fluorescence-activated cell sorter (FACS) (FACSCalibur; BD Biosciences). Data acquisition and analysis were performed by using Cell Quest software (Becton Dickinson, Franklin Lakes, NJ).

**BrdU Labeling and Seeding of ADSCs onto SIS Grafts.** ADSCs (≈60% confluent) were labeled with BrdU at 20 μmol/L concentration for 48 h at 37 °C and then seeded onto the mucosal side of SIS by placing a cell suspension ($1 \times 10^7$ cells per mL) onto the matrix, and then the culture medium was added 4 h later. After 24 h, the SIS-ADSC grafts were placed on the cell culture inserts (Falcon; BD Biosciences) at the interface between the culture medium and a $CO_2$-rich environment. The medium was changed every 2 d for a week to allow for cell adhesion. Hematoxylin/eosin staining was used to evaluate the status of the cell–matrix complex.

**TA Reconstruction.** Animals were divided into four groups ($n$ = 8 per group): control; sham operated; rats undergoing TA incision and grafting with SIS; and rats undergoing TA incision and grafting with SIS-ADSC. The surgical procedures were conducted under anesthesia (i.p. injection of 50 mg/kg sodium pentobarbital). After a circumcision incision to deglove the penis, a rubber band was applied at the base of the penis to provide a blood-free operative field. To protect cavernous nerves from excision or injuries, all experimental excisions for grafting were performed on the lateral sides of the TA. A 0.5-cm incision was then performed through both lateral sides of the TA of the penis. In the sham-operated animals of group 2, the incision was closed by using 8-0 nylon suture. For groups 3 and 4, a 10-$mm^2$ SIS or stem cell-seeded SIS (5 mm × 2 mm) was interpositioned and sutured with 8-0 nylon. The rubber band was then removed, and the skin was closed with 4.0 interrupted absorbable sutures (Fig. 2).

**Measurement of Erectile Response.** Eight weeks after grafting or sham operation, all animals underwent erectile response measurement as described in *SI Text*.

**Penile Size Measurements and Masson's Trichrome Staining.** The penises of all groups were grossly examined for length and diameter. The penile length in both flaccid and at peak erection was measured from the tip of the glans penis to the midpoint of the ischial arch and the diameter from the middle of the body of the penis by using a caliper. The penises were dissected immediately thereafter. The part containing the graft was harvested and placed in O.C.T. compound, frozen rapidly on liquid nitrogen vapor and sectioned at 8 μm for analysis. The sections were stained with Masson's trichrome, which determines the relative proportion of collagen to stromal smooth muscle. The histological examination and the degree of penile fibrosis were evaluated and scored in a blinded fashion as we described (2). The evaluation included architecture and thickness of the TA, arrangement of elastic fiber-lattice framework, and collagen orientation and deposition.

**qRT-PCR Analysis.** The details of qRT-PCR conditions and primer sequences are described in *SI Text* and Table S1.

**Immunofluorescence (IF).** Full details of the IF analysis are given in *SI Text*.

**Western Blot Analysis.** NOS isoforms protein expression in the corpus cavernosum was examined by immunoblotting as described in *SI Text*.

**Statistical Analysis.** Data were presented as mean ± SEM. Comparison between two means was performed with an unpaired Student $t$ test. Analysis of variance (ANOVA) with Fisher's protected least significant difference and Bonferroni–Dunn post hoc analysis were used to detect comparisons of more than two means. Statistical analysis was performed at a 0.05 level of significance.

**ACKNOWLEDGMENTS.** We thank Dr. Zhong Wang (Department of Urology, Medical College of Shanghai Jiaotong University, China) for his excellent technical assistance and Ms. Stephanie McAllister for editing the manuscript. The study was partially supported by "Six Peak Talents" High-Level Personnel Foundation of Jiangsu Province Grant 2009D69 and Nantong Scientific Project Grant S2009036 for L.M. fellowship training in the United States.

1. Lue TF (2000) Erectile dysfunction. *N Engl J Med* 342:1802–1813.
2. Leungwattanakij S, Bivalacqua TJ, Yang DY, Hyun JS, Hellstrom WJ (2003) Comparison of cadaveric pericardial, dermal, vein, and synthetic grafts for tunica albuginea substitution using a rat model. *BJU Int* 92:119–124.
3. Gur S, Ma L, Hellstrom WJ (2011) Current status and new developments in Peyronie's disease: Medical, minimally invasive and surgical treatment options. *Expert Opin Pharmacother* 12:931–944.
4. Kadioglu A, et al. (2007) Graft materials in Peyronie's disease surgery: A comprehensive review. *J Sex Med* 4:581–595.
5. Phinney DG, Prockop DJ (2007) Mesenchymal stem/multi-potent stromal cells (mscs): The state of transdifferentiation and modes of tissue repair - current views. *Stem Cells* 25:2896–2902.
6. Gong Z, Niklason LE (2008) Small-diameter human vessel wall engineered from bone marrow-derived mesenchymal stem cells (hMSCs). *FASEB J* 22:1635–1648.
7. Bernardo ME, et al. (2007) Optimization of *in vitro* expansion of human multipotent mesenchymal stromal cells for cell-therapy approaches: Further insights in the search for a fetal calf serum substitute. *J Cell Physiol* 211:121–130.
8. Lazarus HM, et al. (2005) Cotransplantation of HLA-identical sibling culture-expanded mesenchymal stem cells and hematopoietic stem cells in hematologic malignancy patients. *Biol Blood Marrow Transplant* 11:389–398.
9. Yamada Y, et al. (2004) Autogenous injectable bone for regeneration with mesenchymal stem cells and platelet-rich plasma: Tissue-engineered bone regeneration. *Tissue Eng* 10:955–964.
10. Knoll LD (2007) Use of small intestinal submucosa graft for the surgical management of Peyronie's disease. *J Urol* 178:2474–2478, discussion 2478.
11. Eltahawy EA, Virasoro R, McCammon KA, Schlossberg SM, Jordan GH (2006) Management of Peyronie's disease using dermal or porcine small intestinal submucosa (SIS) grafts. *J Urol* 175:suppl 321, abstract 996.
12. John T, Bandi G, Santucci R (2006) Porcine small intestinal submucosa is not an ideal graft material for Peyronie's disease surgery. *J Urol* 176:1025–1028, discussion 1029.
13. Sievert KD, Tanagho EA (2000) Organ-specific acellular matrix for reconstruction of the urinary tract. *World J Urol* 18:19–25.
14. Seong JM, et al. (2010) Stem cells in bone tissue engineering. *Biomed Mater* 5:062001.
15. Lin CS, et al. (2010) Defining adipose tissue-derived stem cells in tissue and in culture. *Histol Histopathol* 25:807–815.
16. Nakagami H, et al. (2006) Adipose tissue-derived stromal cells as a novel option for regenerative cell therapy. *J Atheroscler Thromb* 13:77–81.
17. Albersen M, et al. (2010) Injections of adipose tissue-derived stem cells and stem cell lysate improve recovery of erectile function in a rat model of cavernous nerve injury. *J Sex Med* 7:3331–3340.
18. Kovanecz I, et al. (2008) Chronic daily tadalafil prevents the corporal fibrosis and veno-occlusive dysfunction that occurs after cavernosal nerve resection. *BJU Int* 101:203–210.
19. Lin G, et al. (2010) Pentoxifylline attenuates transforming growth factor-beta1-stimulated elastogenesis in human tunica albuginea-derived fibroblasts part 2: Interference in a TGF-beta1/Smad-dependent mechanism and downregulation of AAT1. *J Sex Med* 7:1787–1797.
20. Kilroy GE, et al. (2007) Cytokine profile of human adipose-derived stem cells: Expression of angiogenic, hematopoietic, and pro-inflammatory factors. *J Cell Physiol* 212:702–709.
21. Lee EY, et al. (2009) Hypoxia-enhanced wound-healing function of adipose-derived stem cells: Increase in stem cell proliferation and up-regulation of VEGF and bFGF. *Wound Repair Regen* 17:540–547.
22. Cai L, et al. (2007) Suppression of hepatocyte growth factor production impairs the ability of adipose-derived stem cells to promote ischemic tissue revascularization. *Stem Cells* 25:3234–3243.
23. Kane AJ, et al. (2001) Inducible nitric oxide synthase (iNOS) activity promotes ischaemic skin flap survival. *Br J Pharmacol* 132:1631–1638.
24. Kendirci M, et al. (2005) Poly(Adenosine diphosphate-ribose) polymerase inhibition preserves erectile function in rats after cavernous nerve injury. *J Urol* 174:2054–2059.
25. Bivalacqua TJ, et al. (2000) A rat model of Peyronie's disease associated with a decrease in erectile activity and an increase in inducible nitric oxide synthase protein expression. *J Urol* 163:1992–1998.
26. Jesmin S, et al. (2003) Diminished penile expression of vascular endothelial growth factor and its receptors at the insulin-resistant stage of a type II diabetic rat model: A possible cause for erectile dysfunction in diabetes. *J Mol Endocrinol* 31:401–418.
27. Donnenberg VS, et al. (2010) Localization of CD44 and CD90 positive cells to the invasive front of breast tumors. *Cytometry B Clin Cytom* 78:287–301.